**INP5-3L**
***Late-News Paper***

# Influence of Photocurrent Diffusion of Organic Photodetector to Fingerprint-On-Display Using Pinhole Imaging Technique

**Muhamad Affiq Bin Misran[1] and Reiji Hattori[1,2]**

misran.muhamad.458@s.kyushu-u.ac.jp
[1]Department of Applied Science for Electronics and Materials, Interdisciplinary Graduate School of Engineering Sciences, Kyushu University, Fukuoka 816-8580, Japan
[2]Global Innovation Center, Kyushu University, Fukuoka 816-8580, Japan
Keywords: pinhole imaging technique, organic photodetectors, photocurrent diffusion, organic image sensor.

**ABSTRACT**

*Fingerprint on Display (FOD) has been widely studied for large area displays. It can be achieved through solution-processable organic photodetectors. Thus, we analyzed the light distribution from a pinhole structure onto the sensor surface and diffusion photocurrent between adjacent pixels for the organic image sensor.*

## 1 Introduction

Researchers have proven and incorporated optical and ultrasonic sensors into Fingerprint on Display (FOD) technology in recent years, as evidenced by various research projects [1-4]. The size and location of the module determine the ultrasonic sensor's detection range. In contrast, the optical sensing approach can fully use novel opportunities like full-display sensing. It is feasible since most researchers have concentrated on the organic photodiode (OPD), one of the promising candidates for the image-sensing component of the biometric authentication system [1,5–8]. Compared to inorganic photodetector (PD), OPDs have several advantages. Consider the processibility of the solution and the low process temperature. These enable the construction of large-area photodetector arrays at meager costs on a thin plastic substrate.

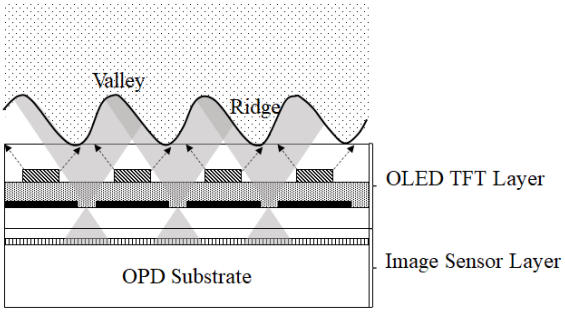


**Fig. 1 FOD principle.**

Lenses and collimators are used in the majority of optical FOD approaches that are currently on the market. However, the thickness of the display panel will increase due to the lenses and collimators and integrating them with the panel is not a simple task. Under this consideration, numerous panel producers are striving to develop an alternative way to solve this issue based on the pinhole matrix imaging approach [9,10]. Pinhole imaging is well known for producing enormous images with a straightforward structure. However, there is currently a deficiency of knowledge regarding the FOD application of this approach. The pinhole imaging system depends on several factors, including pinhole diameter and the distance between the pinhole and the sensor.

As a result, we examined the light distribution from the pinholes to the sensor layer in this work. Additionally, using the spin-coating method on solution processable OPDs, we examined the diffusion photocurrent between neighboring OPD. This procedure will cover the entire region in a continuous photoactive layer. Therefore, there is a higher tendency for photocurrent diffusion between adjacent electrodes to increase.

## 2 Experiment

There were two phases to the experiments. The light distribution beneath the pinhole area was observed using analysis modeling, as shown in Fig. 2. The same model was used to examine the light distribution from numerous pinholes.

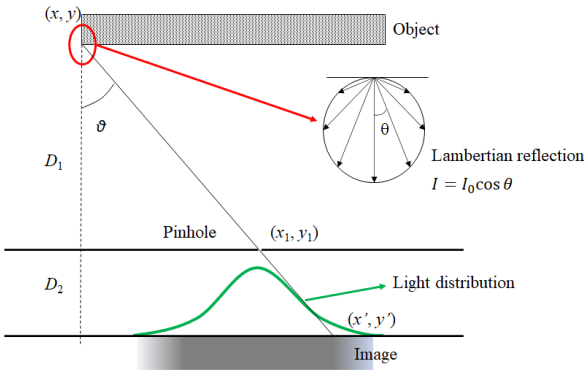


**Fig. 2 Pinhole mechanism.**

The second phase of the experiments was done by measuring the crosstalk photocurrent between adjacent OPDs using the structure shown in Fig. 3. The fabrication process was discussed elsewhere [11]. The fabricated OPDs were bottom side illuminated structures. During illumination from the bottom side, only the

exposed OPDs were properly illuminated, and the Mo layer protected the covered OPDs.

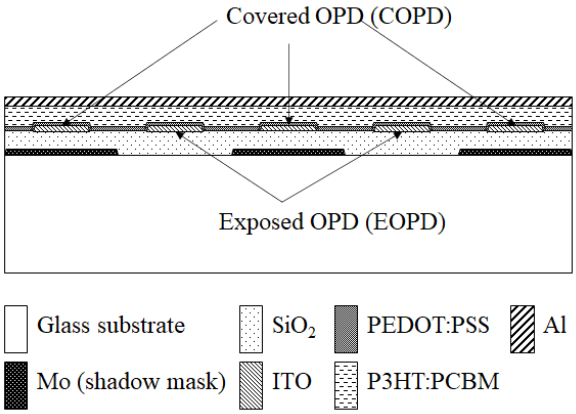


**Fig. 3 Interdigitated electrodes (IDEs) OPDs.**

## 3 Results and discussion

The light distribution analysis analyzed three pinholes with a 1 mm pitch. The distance between the object and the pinhole ($D_1$) was fixed at 500 µm. Whereas 100 µm for the distance from the pinhole to the sensor surface ($D_2$).

The crosstalk photocurrent was investigated by fabricating the devices with the distance between the edge of both covered and exposed electrodes changed to 2 µm, 4 µm, 10 µm, and 20 µm. The diffusion photocurrent was studied by varying the edge of the shadow mask to the edge of the covered electrode with 1 µm, 2 µm, 5 µm, and 10 µm.

### 3.1 Light distribution

In this analysis, three pinholes with a 1 mm pitch were analyzed. The $D_1$ was fixed at 500 µm. Whereas 100 µm for the $D_2$.

The distribution of current intensity from three pinholes onto the sensor's surface is shown in Fig. 4. On the sensor's surface, the area just beneath the pinhole had the highest intensity. This intensity decreased as the sensor point moved away from the center. Other pinholes also showed similar pattern.

The overlapped region of the distribution from other pinholes is also shown in Fig. 4. One of the optical crosstalk sources, the high light intensity at the overlapped region, needs to be adequately addressed. This optical crosstalk will give incorrect information throughout the biometric recognition process, lowering the system's dependability.

Decreasing the sensor pixel size is one method for reducing this optical crosstalk from other pinholes. As seen in Fig. 4, it can be carried out based on the distribution of light intensity at the effective region. According to the FBI standard, a biometric authentication system's minimum resolution must be 500 pixels per inch (ppi). This specification requires a resolution of 50 µm with 20 pixels or more every 1000 µm.

In this analysis, the pinholes were assumed to be a single point, and $D_1$ and $D_2$ were fixed for simplicity. However, diffraction may occur through this system. Thus, additional factors such as pinhole diameter and thickness need to be taken care of to enhance the image and reduce the geometrical effect of this system on the image produced.

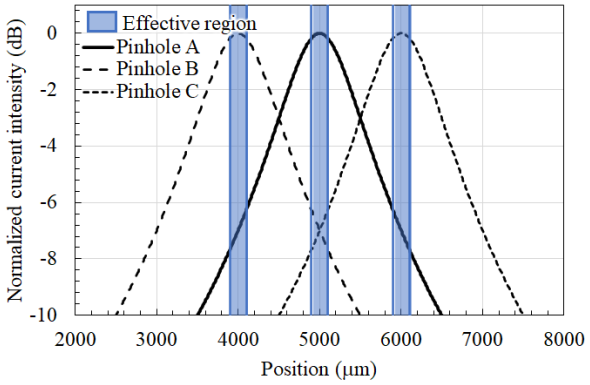


**Fig. 4 Normalized current density distribution from adjacent pinholes to the sensor surface.**

### 3.2 Crosstalk photocurrent

The crosstalk photocurrent at different light intensities onto different distances of electrodes between the exposed area to the covered electrode was plotted, as shown in Fig. 5. The crosstalk photocurrent values were normalized to the electrode width, which is 100 µm It shows that the crosstalk photocurrent increased when the light intensities increased at 10 µW/cm$^2$, 30 µW/cm$^2$ and 60 µW/cm$^2$. At different distances between the exposed and covered electrodes, the crosstalk photocurrent has slight differences but is almost constant within a similar magnitude. In this study, the reflection of light within the thin film layer across the neighboring devices was assumed to be negligible. It can be supported by our findings based on Fig. 5, as the distance between the exposed areas and covered electrodes did not significantly impact the diffusion photocurrent.

The range of 5-10 nm for the exciton diffusion length in organic semiconductor (OSC) materials is well known [12]. Surprisingly, the photocurrent was still noticeable at 10 µm between the hidden electrodes and the exposed regions. It might result from the shared bulk-heterojunction (BHJ) layer from the OSC materials on the entire surface. The longer exciton diffusion length is suspected due to the longer lifetime of the exciton itself. During testing, the continuous illumination process mainly attributed the diffused excitons to the covered electrodes from the exposed regions.

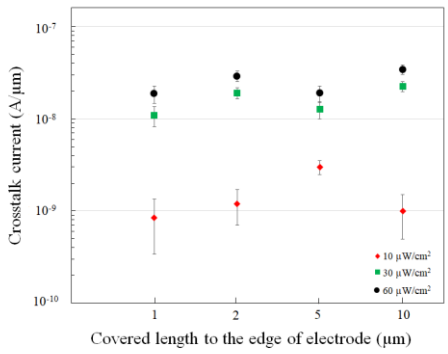


**Fig. 5 Crosstalk photocurrent**

As mentioned earlier, the biometric authentication system requires a minimum resolution of 50 µm. According to Fig. 5, the separation between adjacent OPDs should be more than 10 µm to prevent the crosstalk photocurrent. It implies that the size of the OPDs must be decreased to account for the requirement. However, Fig. 7 also demonstrates that the 1 µm distance has a crosstalk photocurrent almost identical to the 10 µm distance.

Despite the noticeably low crosstalk photocurrent discovered in this study, adequate isolation between nearby pixels is required for the spin-coating process to further limit the exciton diffusion, particularly in adjoining OPDs. Several topologies for the photoactive layer, including the planar heterojunction and ordered heterojunction, can be used further to analyze the exciton diffusion study between adjacent pixels.

## 4 Conclusions

As a result of its simplicity and viability for the large-area sensing display, we have explored the FOD structure based on the pinhole imaging technique and the photocurrent diffusion from the exposed region to the covered electrodes from the fabricated OPDs through the spin-coating process. The trade-off between the geometry of the pinhole and the diffraction caused by each pinhole is one of the crucial aspects that can be considered for future improvement in the context of the pinhole analysis.

To lessen the crosstalk photocurrent caused by the diffusion photocurrent from the neighboring OPDs, the spacing between the OPDs should be larger than 10 µm. As the minimum requirement of a single pixel size for the image sensor used for the fingerprint authentication is about 50 µm, increasing the distance between OPDs to more than 10 µm will reduce the image sensor size and vice versa. Despite the low crosstalk photocurrent found in this investigation, suitable isolation layer is still required. Plus, various structures of the photoactive layer can be used to study this effect further, such as planar and ordered heterojunctions.

## References


[1] T. Kamada *et al.*, “OLED display incorporating organic photodiodes for fingerprint imaging,” *J Soc Inf Display*, vol. 27, no. 6, pp. 361–371, Jun. 2019, doi: 10.1002/jsid.786.

[2] Y. Kwon *et al.*, “A Low Noise Read-Out IC with Gate Driver for Full Front Display Area Optical Fingerprint Sensors,” in *2020 IEEE Symposium on VLSI Circuits*, Honolulu, HI, USA, Jun. 2020, pp. 1–2. doi: 10.1109/VLSICircuits18222.2020.9162909.

[3] C. Peng, M. Chen, H. Wang, J. Shen, and X. Jiang, “P(VDF-TrFE) Thin-Film-Based Transducer for Under-Display Ultrasonic Fingerprint Sensing Applications,” *IEEE Sensors J.*, vol. 20, no. 19, pp. 11221–11228, Oct. 2020, doi: 10.1109/JSEN.2020.2997375.

[4] C. Peng, M. Chen, and X. Jiang, “Under-Display Ultrasonic Fingerprint Recognition With Finger Vessel Imaging,” *IEEE Sensors J.*, vol. 21, no. 6, pp. 7412–7419, Mar. 2021, doi: 10.1109/JSEN.2021.3051975.

[5] Y. Qin, H. Wang, and Y. Liu, “P-215: Organic-Inorganic Hybrid Thin-film Photo-detector for Fingerprint Recognition,” *SID Symposium Digest of Technical Papers*, vol. 49, no. 1, pp. 1604–1606, May 2018, doi: 10.1002/sdtp.12466.

[6] D. Tordera *et al.*, “A High-Resolution Thin-Film Fingerprint Sensor Using a Printed Organic Photodetector,” *Adv. Mater. Technol.*, vol. 4, no. 11, p. 1900651, Nov. 2019, doi: 10.1002/admt.201900651.

[7] D. Tordera *et al.*, “Vein detection with near-infrared organic photodetectors for biometric authentication,” *J Soc Inf Display*, vol. 28, no. 5, pp. 381–391, May 2020, doi: 10.1002/jsid.891.

[8] H. Akkerman *et al.*, “Integration of large-area optical imagers for biometric recognition and touch in displays,” *J Soc Inf Display*, vol. 29, no. 12, pp. 935–947, Dec. 2021, doi: 10.1002/jsid.1060.

[9] W.-F. Zhou *et al.*, “76-1: *Invited Paper:* A New Full Screen Flexible AMOLED Solution with Fingerprint,” *SID Symposium Digest of Technical Papers*, vol. 49, no. 1, pp. 1014–1016, May 2018, doi: 10.1002/sdtp.12231.

[10] Y. Zeng, F. Lu, Q. Yao, H. Yu, Q. Zhang, and X. Su, “7.4: Investigation of Moiré Interference in Pinhole Matrix Fingerprint on Display Technology,” *SID Symposium Digest of Technical Papers*, vol. 52, no. S1, pp. 49–52, Feb. 2021, doi: 10.1002/sdtp.14370.

[11] M. A. B. Misran, R. Khan, A. Bilgaiyan, and R. Hattori, “Photocurrent diffusion of organic photodetector between pixels for fingerprint sensor by using interdigitated electrodes,” *Jpn. J. Appl. Phys.*, vol. 61, no. 10, p. 104001, Oct. 2022, doi: 10.35848/1347-4065/ac89c1.

[12] O. V. Mikhnenko, P. W. M. Blom, and T.-Q. Nguyen, “Exciton diffusion in organic semiconductors,” *Energy Environ. Sci.*, vol. 8, no. 7, pp. 1867–1888, 2015, doi: 10.1039/C5EE00925A.